Chapter 15
Assessing the Importance of Contact Joints Relative to Other Sources of Uncertainty in Dynamic Substructuring

Samuel Choi, Manuel Vega, Tyler Alvis, and Teresa Portone

Abstract Dynamic substructuring enables the analysis of complex mechanical systems by partitioning them into system subcomponents. These subcomponents can be either modeled as numerical or experimental pieces. There are many sources of uncertainty in the dynamic substructuring process, including those arising from numerical modeling choices. Contact joint modeling choices specifically may be influential, especially for high-frequency dynamic quantities of interest. This paper presents a sensitivity analysis to assess the importance of contact joint modeling relative to other sources of uncertainty in the dynamic substructuring process. The study focuses on SEM's frame-wing benchmark structure, with the aim of providing suggestions to improve the fidelity of dynamic substructuring simulations.

Keywords Dynamic substructuring · Contact joint modeling · Uncertainty Quantification · SEM Round Robin · Contact

Introduction

Modal analysis provides critical insight into the dynamic behavior of engineered systems. However, numerous uncertainties can influence the outcomes of this analysis in practice. Traditionally, modal analysis involves testing the complete system as a unified entity, meaning that any modifications necessitate a comprehensive rebuild and retesting of the entire system. In this context, numerical modal analysis serves as a complementary approach, utilizing computational methods such as finite element analysis (FEA) to determine the dynamic characteristics of mechanical systems [1]. This technique involves discretizing a structure into smaller elements, enabling the calculation of natural frequencies, mode shapes, and damping ratios.

Dynamic substructuring offers an alternative method when experimental analysis of the entire structure is impractical, particularly in cases where the structure is too large or complex. In some instances, it may not be feasible to experimentally test the entire structure, leading to scenarios where part of the structure is modeled experimentally while other parts are modeled numerically [2, 3, 4]. Dynamic substructuring enables the integration of subcomponents to accurately predict the dynamics of the assembled system, thereby reducing both testing time and associated costs.

Despite its advantages, dynamic substructuring is accompanied by various uncertainties. These uncertainties can arise from multiple sources, including measurement errors when using experimental data for a subcomponent, input uncertainties in finite element (FE) models for numerical data, and ambiguous choices in the substructuring process—such as where to apply constraints, how many constraints to implement, and how many modes to include from each subcomponent. Understanding the influence of these uncertainties on our quantities of interest is essential for assessing the confidence we can place in the results. Additionally, identifying the key factors driving uncertainty is crucial for focusing efforts on their reduction.

Samuel Choi · Manuel Vega
Verification, Validation, and Uncertainty Quantification Processes Department, Sandia National Laboratories, Albuquerque, NM 87123
e-mail: samchoi@sandia.gov; mavega@sandia.gov

Tyler Alvis
Analytical Structural Dynamics Department, Sandia National Laboratories, Albuquerque, NM 87123
e-mail: tylalvi@sandia.gov

Teresa Portone
Optimization and Uncertainty Quantification Department, Sandia National Laboratories, Albuquerque, NM 87123
e-mail: tporton@sandia.gov

Walter D'Ambrogio, et al. (eds.), *Dynamic Substructuring & Transfer Path Analysis, Vol. 4*, Conference Proceedings of the Society for Experimental Mechanics Series, https://doi.org/10.13052/97887-438-0149-8_15

Real-world contact surfaces are rarely flat, and when a surface is fastened by multiple bolts, uneven pressure distribution occurs due to variations in surface roughness and torquing specifications. These variations can significantly affect the modal characteristics of the system. In [5] these joints were modeled as spring contacts tuned to experimental data. In this paper, we will discuss the results that compare the importance of contact joint modeling relative to other sources of uncertainty within the dynamic substructuring framework.

Last year, we investigated the impact of FE model input uncertainties on dynamic substructuring quantities of interest in the context of the Dynamic Substructuring SEM Round Robin problem [6]. However, we did not explore the effects of substructuring uncertainties, such as the number of modes to include from each subcomponent, nor did we examine the implications of joint model choices. Joint modeling presents particular challenges due to the complex interactions at the interfaces, which can significantly influence the overall dynamic response of the system. This year, we expand our investigation to incorporate these additional sources of uncertainty, aiming to provide a more comprehensive understanding of their effects on dynamic substructuring outcomes.

Background

The objective of dynamic substructuring is to analyze a multi-component structure by breaking it down into smaller, more manageable subcomponents or substructures. One method to do this is to use a transmission simulator [7, 8]. Let's assume we have two subcomponents, A and B. If A and B share a common fixture, they can be connected via this fixture. This common fixture, known as a transmission simulator (TS), facilitates the analysis of the integration between subcomponents A and B. The TS acts as a bridge, enabling the study of combined behavior of A and B. This concept is illustrated in Figure 1.

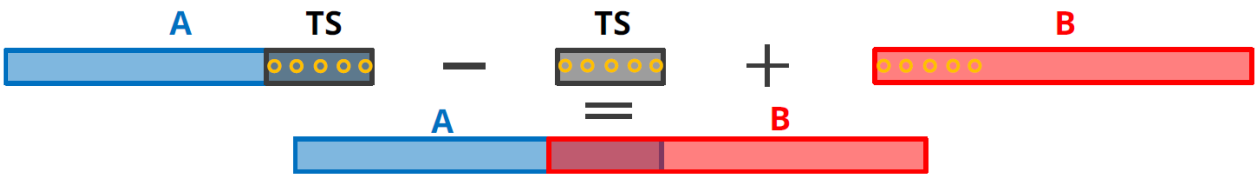

Fig. 1 Visualization of Transmission Simulator (TS)[5]

To get the modal characteristics, we have to solve a modal system of equations. The general form of the uncoupled modal equations of motion for a subcomponent is:

$$\mathbf{M}_i\ddot{\mathbf{q}}_i(t) + \mathbf{C}_i\dot{\mathbf{q}}_i(t) + \mathbf{K}_i\mathbf{q}_i(t) = \mathbf{F}_i(t) \tag{1}$$

where:

- $\mathbf{M}_i$ is the mass matrix,
- $\mathbf{C}_i$ is the damping matrix,
- $\mathbf{K}_i$ is the stiffness matrix,
- $\mathbf{q}_i(t)$ is the modal displacement vector,
- $\mathbf{F}_i(t)$ is the external force vector.

Each subcomponent is characterized by a set of uncoupled modal equations, each defined by its own modal characteristics: linear natural frequency (ω), damping ratio (ζ), and mode shape (ϕ). By combining the three equations and moving the mass terms, Equation (1) can be written as Equation (2) in terms of subcomponents A, B and TS. Note that the negative TS terms correlate to the removal of the TS subcomponent in Figure 1.

$$\begin{bmatrix} \mathbf{I}_A & \mathbf{0} & \mathbf{0} \\ \mathbf{0} & \mathbf{I}_B & \mathbf{0} \\ \mathbf{0} & \mathbf{0} & -\mathbf{I}_{TS} \end{bmatrix} \begin{bmatrix} \ddot{\mathbf{q}}_A(t) \\ \ddot{\mathbf{q}}_B(t) \\ \ddot{\mathbf{q}}_{TS}(t) \end{bmatrix} + \begin{bmatrix} \left[\ddots 2\zeta_A\omega_{A_{\cdot\cdot}}\right] & \mathbf{0} & \mathbf{0} \\ \mathbf{0} & \left[\ddots 2\zeta_B\omega_{B_{\cdot\cdot}}\right] & \mathbf{0} \\ \mathbf{0} & \mathbf{0} & -\left[\ddots 2\zeta_{TS}\omega_{TS_{\cdot\cdot}}\right] \end{bmatrix} \begin{bmatrix} \dot{\mathbf{q}}_A(t) \\ \dot{\mathbf{q}}_B(t) \\ \dot{\mathbf{q}}_{TS}(t) \end{bmatrix}$$
$$+ \begin{bmatrix} \left[\ddots \omega^2_{A_{\cdot\cdot}}\right] & \mathbf{0} & \mathbf{0} \\ \mathbf{0} & \left[\ddots \omega^2_{B_{\cdot\cdot}}\right] & \mathbf{0} \\ \mathbf{0} & \mathbf{0} & -\left[\ddots \omega^2_{TS_{\cdot\cdot}}\right] \end{bmatrix} \begin{bmatrix} \mathbf{q}_A(t) \\ \mathbf{q}_B(t) \\ \mathbf{q}_{TS}(t) \end{bmatrix} = \begin{bmatrix} \phi_A^\top \mathbf{F}_A(t) \\ \phi_B^\top \mathbf{F}_B(t) \\ \phi_{TS}^\top \mathbf{F}_{TS}(t) \end{bmatrix} \tag{2}$$

To couple the subcomponent, the TS method enforces constraints on the displacements at a subset of degrees of freedom (DOFs) in subcomponent A and B, ensuring they match those of the TS. These constraints are transformed into modal space using a modal transformation and softened using the pseudo-inverse of the TS shapes [6]. The coordinate transformation $\mathbf{q} = \mathbf{L}\eta$ is used to enforce these constraints, where $\mathbf{L}$ resides in the null space of the modal constraint matrix. A more in-depth description of the math is mentioned in [5]. The aim of this work is to understand the influence of uncertainties in the dynamic substructuring process.

Uncertainty quantification is the process of identifying, characterizing, and quantifying uncertainty in order to reduce uncertainties in mathematical models. Representing real world phenomena in exact terms is nearly impossible. Uncertainties in models arise from two sources: aleatory uncertainties and epistemic uncertainties. Aleatory uncertainties are due to inherent variability in known variables. In the manufacturing of aluminum, the processes of manufacturing and post-treating metals do not produce an exact Young's modulus or density. The reported values are averages derived from samples taken throughout the entire process. Within the same block, due to grain structure, the values exhibit a range, let alone the variance from bar to bar. This variability increases when the composition and post-treatment processes are unknown. Aleatory uncertainties are most often modeled using a probability distribution. In this case, as in the previous study, since only the range is known, a uniform random variable is assumed over this range. On the other hand, epistemic uncertainties arise from the lack of knowledge. An example in dynamic substructuring is interface modeling uncertainties that arise from the lack of knowledge such as the effects of friction or gaps.

In this study, we employed a forward propagation method to analyze the influence of uncertainties on the system under investigation. By evaluating random samples of uncertain inputs, we determined their corresponding outputs, capturing the range of possible outcomes and associated uncertainties. To achieve this, we utilized Latin Hypercube Sampling (LHS) to generate the input samples. FE analysis was conducted using Sierra/SD [9], while dynamic substructuring was performed using the Python library Sdynpy [10]. Uncertainty propagation was carried out using the open-source uncertainty quantification toolkit Dakota [11], with a total of 6,400 samples taken.

Correlation coefficients measures the linear correlation between the input the output. These coefficients range from -1 to 1 where 1 represents a perfect positive linear relationship and -1 represents a perfect negative linear relationship. It is important to note that the Pearson correlation coefficient does not represent the slope of the best-fit line; it only measures the strength and direction of the linear relationship between the variables. Additionally, coefficients may not detect a nonmonotonic or strongly nonlinear dependence of the output on an input. The benefit of using Pearson correlation coefficients over Sobol' indices, for instance, is that they do not require a large sample size.

The Pearson correlation coefficient r between two variables X and Y is defined as follows:

$$r = \frac{\text{Cov}(X, Y)}{\sigma_X \sigma_Y} \tag{3}$$

where:

- $\text{Cov}(X, Y)$ is the covariance between X and Y,
- σ_X is the standard deviation of X,
- σ_Y is the standard deviation of Y.

Methodology

The frame-wing example problem represents a second iteration of modeling the Dynamic Substructuring SEM Round Robin problem [6, 5]. The models and the location of the 4 bolts are displayed in Figure 2. During the initial study, the dynamic substructuring problem modeled the highlighted connection using springs. In this iteration, it is modeled as a contact surface. The initial configuration (i.e., Frame + Thin Wing) featured a frame with a thin wing bolted via four bolts. The thin wing, which served as a transmission simulator, is replaced with a thicker wing.

For the material properties, including Young's modulus and density, known ranges were sourced from Granta MI [12]. Due to the unknown specific composition of the aluminum, a range encompassing a wide range of compositions was used. The ranges are listed in Table 1.

The contact areas were determined by the radii at the four bolt locations, with each bolt having an independent contact radius. The contact constraints were defined by the size of the bolt head on the lower range and the frame on the upper range. Tied contact was employed to join the two surfaces together for the duration of the simulation. This method constrains the

Number of modes were found using the random variable (RV) and Equation (4).

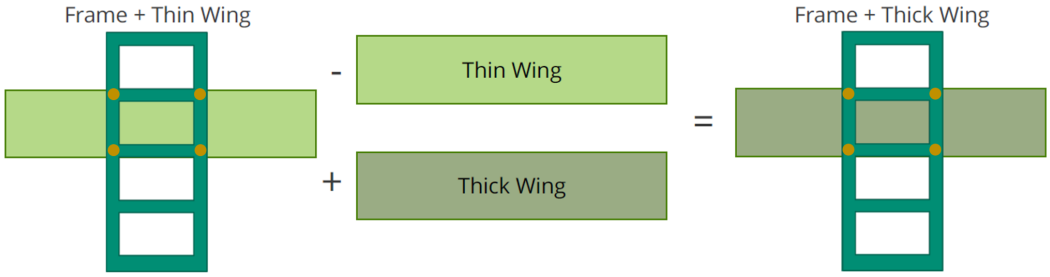

Fig. 2 Visualization of the Model used for Dynamic Substructuring [5]

Table 1 Uncertainty types and their corresponding uncertain input distributions.

Uncertainty Type	Uncertain Input	Distribution
Material properties	Young's modulus $E_{\text{al}}, E_{\text{al\_wing\_thick}}, E_{\text{al\_wing\_thin}}$ [GPa]	$\mathrm{U}[66.6, 74.5]$
	Density $\nu_{\text{al}}, \nu_{\text{al\_wing\_thick}}, \nu_{\text{al\_wing\_thin}}$ [kg/m³]	$\mathrm{U}[2694.3, 2824.6]$
Geometric properties	Contact radius R_1, R_2, R_3, R_4 [mm]	$\mathrm{U}[4.19, 5.46]$
Substructuring	Number of modes $RV_{\text{ThinFrame}}, RV_{\text{Thick}}, RV_{\text{Thin}}$ [-]	$\mathrm{U}[0, 1]$[1]

nodes on one surface to match the displacement of the corresponding nodes on the opposing surface. Figure 3(a) shows the maximum contact area, with the red section indicating the region where contact occurs. Conversely, Figure 3(b) illustrates the minimum contact area, also highlighted in red. The green sections indicate partial contact, while the blue sections indicate no contact. The irregular shapes of the other sections are due to meshing artifacts and should be disregarded.

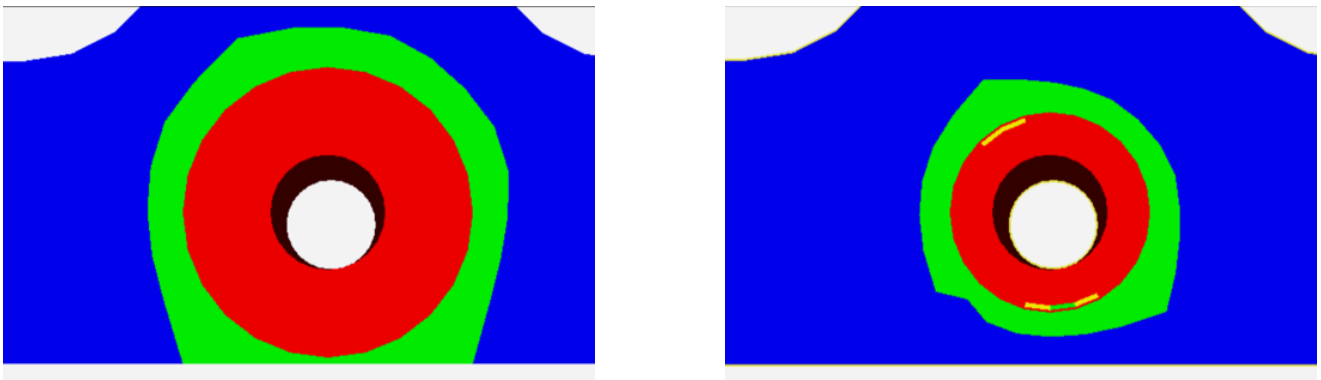

(a) Maximum contact radius

(b) Minimum contact radius

Fig. 3 Minimum and maximum contact area

To determine the appropriate number of modes for each configuration, we considered several methodologies, including manual selection and the use of a loss function. However, given the complexity and the reliance on subject matter expert (SME) judgment typically required for mode selection, we opted for sampling and systematic evaluation of a wide range of possible modes. For each number of mode variable, a uniform random variable between 0 and 1 is sampled. This uniform random variable is used to select a point within predefined bounds. The actual number of modes selected for substructuring is then set based on these bounds and the sampled uniform random variable. For the frame plus thin wing configuration, the bounds are defined to ensure that the number of modes includes at least one mode at 1600 Hz in the shape set, with an upper limit of 50.

The Number of Modes (Nmodes) value is calculated using the formula:

$$\text{Nmodes} = U \times (\text{upper bound} - \text{lower bound}) + \text{lower bound} \tag{4}$$

where U is the sampled uniform random variable between 0 and 1. For the thick wing and thin wing configurations, the lower bound is set to 7 (accounting for 6 rigid modes plus one flexible mode), and the upper bound is the number of modes selected for the frame plus thin wing configuration. Nmodes value is then rounded to the nearest integer.

Before conducting a detailed analysis, we first investigated the effects of uncertainties in the FE model. There are a few key differences between the FE model and the experimental model: the FE model utilized simplified bolts with the threads removed and without nuts, whereas the experimental model featured an aluminum frame with steel threaded inserts and standard bolts. This analysis was performed using Sierra/SD FE models [9]. A Modal Assurance Criterion (MAC) was calculated between the mode shapes obtained from each of the subcomponent FEM models and the experimental mode shapes. The resulting MAC values are displayed in Figure 4. Darker squares represent higher MAC scores, meaning there is a stronger similarity between the numerical and experimental mode shapes. This indicates a higher degree of similarity in the modal shapes, suggesting that the modeled FE models closely match the experimental results. The high scores across the diagonal for both the thin wing and thick wing configurations indicate a similarity in all mode shapes. However, in the frame plus thin wing configuration, the MAC score drops along the diagonal as the frequency increases, particularly around the frequency of 1400 Hz. The first 44 bending modes were taken into consideration.

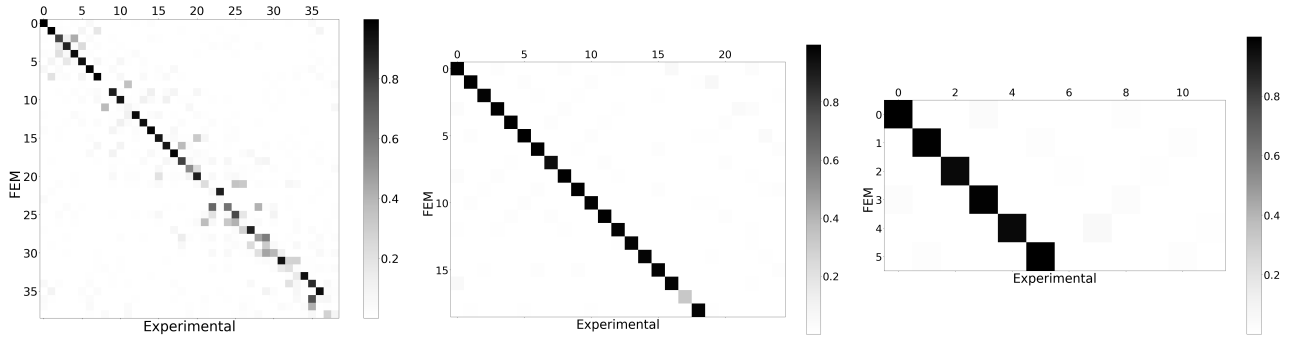

(a) MAC: Frame + Thin Wing (b) MAC: Thin Wing (c) MAC: Thick Wing

Fig. 4 Modal Assurance Criterion for subcomponents of dynamic substructuring

To gain deeper insights into the input parameters, a Pearson correlation analysis was performed to assess the relationship between the input parameters (i.e., model parameters and substructuring parameters) and the natural frequencies across each of the considered flexible modes. Figure 5 illustrates the correlation coefficients between the input parameters and the non-rigid natural frequencies, with dark red indicating a perfect positive correlation and dark blue representing a perfect negative

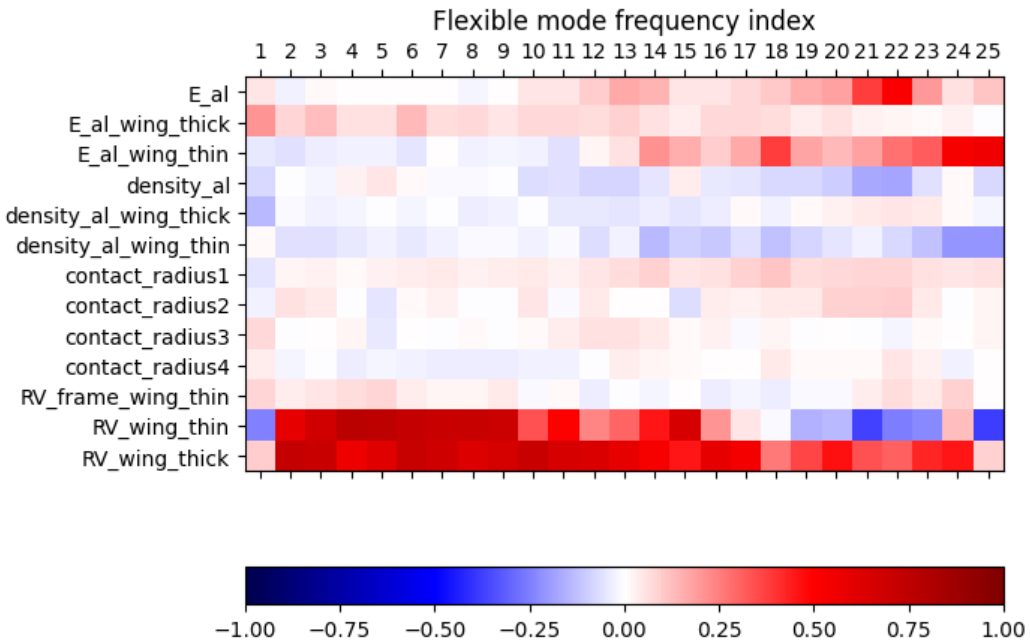

Fig. 5 Correlation coefficients across flexible modes

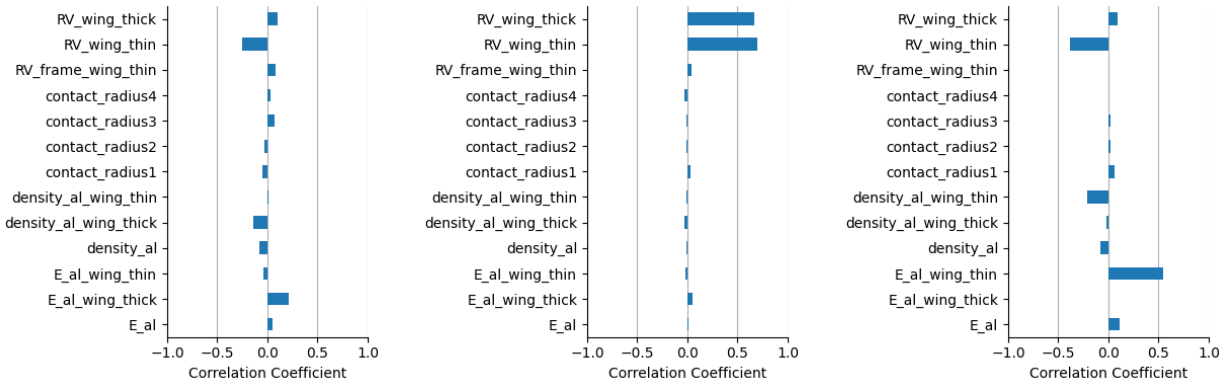

(a) Flexible mode 1 (b) Flexible mode 9 (c) Flexible mode 25

Fig. 6 Correlation coefficient for individual flexible modes

correlation. In most flexible modes, a significant positive correlation was observed between the random variables selected for the substructuring of the removed thin wing and the added thick wing. This indicates that variations in the substructuring parameters are linked to changes in the natural frequencies, underscoring the importance of these variables in the system's dynamic behavior. Moreover, at higher frequencies, the correlation between the number of modes selected from the thin wing and the natural frequencies turns negative. Additionally, Young's modulus in the thin wing shows a stronger positive correlation with the higher natural frequencies.

Visualizing the correlation coefficients for flexible modes 1, 9, and 25 individually highlights representative patterns, as shown in Figure 6(a). The correlation coefficients for the first flexible mode (or first natural frequency) do not exhibit high values, indicating a lack of strong linear correlation with the input variables. In contrast, Figure 6(b) demonstrates a strong correlation between the natural frequency and the number of modes chosen when removing the thin wing and adding the thick wing, suggesting that substructuring parameters play a significant role in this natural frequency. Furthermore, Figure 6(c) illustrates that for the 25th natural frequency, there is a strong negative correlation between the natural frequency and the Young's modulus of the thin wing, highlighting the influence of material properties on the dynamic behavior of the system at this frequency.

Conclusion

In the previous study [5], the number of modes selected for substructuring was not included. We predicted that this would be a major source of uncertainty, and this was verified during this study. Based on this study, the other variables did not have a significant effect compared to the number of modes selected. The correlation coefficients between the number of modes and other variables were found to be close to zero, indicating minimal association under the current conditions. This may change at higher frequencies as the influence of the number of modes diminishes. It is also possible that the high correlation coefficient of mode selection could obscure the correlations between other variables and the natural frequencies.

We could validate our selection of modes because we can compare the substructured model against a full model of a system with the updated component (e.g., after adding component B and removing component A). However, in scenarios where full validated models are unavailable, validating the substructured model becomes challenging. Therefore, we need to find a method to select the modes more intelligently. This will help prevent the dominant effect of uncertainty in mode selection from overshadowing other uncertainties. Historically, modes have been manually picked or sampled from a distribution, but these approaches may not be optimal or feasible.

Although contact radius don't seem to have a high correlation for this model, models that incorporate a greater number of joints or more complex geometries could potentially exhibit different behaviors. The increased complexity may introduce additional interactions and dependencies among the variables, which could lead to a stronger correlation between contact uncertainties and natural frequencies. Therefore, further exploration into models with varying configurations and joint arrangements is warranted. This could enhance our understanding of how contact conditions influence dynamic performance and may reveal critical insights that were not apparent in this study.

Dynamic substructuring and its associated uncertainties remain the subject of ongoing work. We plan on conducting more samples and comparing correlations using other methods, such as Sobol indices. Future work involves increasing the contact radius and studying the effects this has on the modal frequency. In the current study, the contacts were circular and of uniform shape; this was to simplify initial calculations. However, in practice, contact is rarely nicely rounded and constant. Many times, contact occurs in other locations along the frame, not just near the bolts. Additionally, future research will focus on determining the effects of these uncertainties on the frequency response functions, which will be the major focus of our future work.

Acknowledgments

This article has been authored by an employee of National Technology & Engineering Solutions of Sandia, LLC under Contract No. DE-NA0003525 with the U.S. Department of Energy (DOE). The employee owns all right, title and interest in and to the article and is solely responsible for its contents. The United States Government retains and the publisher, by accepting the article for publication, acknowledges that the United States Government retains a non-exclusive, paid-up, irrevocable, worldwide license to publish or reproduce the published form of this article or allow others to do so, for United States Government purposes. The DOE will provide public access to these results of federally sponsored research in accordance with the DOE Public Access Plan https://www.energy.gov/downloads/doe-public-access-plan.

References

1. Black, J.K., Callis, S.J., Feizy, A., Johnson, C.L., Lieven, N.A., and Vega, M.A. "A simplified finite element joint model updated with experimental modal features". In *Proceedings of the Society for Experimental Mechanics Annual Conference and Exposition*, pages 107–123. Society for Experimental Mechanics, Springer (2023)
2. De Klerk, D., Rixen, D.J., and Voormeeren, S. "General framework for dynamic substructuring: history, review and classification of techniques". *AIAA journal*, 46(5):1169–1181 (2008)
3. Vega, M.A., Schellenberg, A.H., Caudana, H., and Mosqueda, G. "Implementation of real-time hybrid shake table testing using the ucsd large high-performance outdoor shake table". *International Journal of Lifecycle Performance Engineering*, 4(1-3):80–102 (2020)
4. Allen, M.S., Gindlin, H.M., and Mayes, R.L. "Experimental modal substructuring to estimate fixed-base modes from tests on a flexible fixture". *Journal of Sound and Vibration*, 330(18-19):4413–4428 (2011)
5. Portone, T., Roettgen, D., Neal, K., and Debusschere, B. "A preliminary quantification of uncertainties in dynamic substructuring and the frame-wing problem". In *Proceedings of the IMAC Conference*. Society for Experimental Mechanics (2024)
6. Roettgen, D.R., Lopp, G.K., and Linderholt, A. "Technical division benchmark structure for dynamic substructuring.". Technical report, Sandia National Lab.(SNL-NM), Albuquerque, NM (United States) (2020)
7. Mayes, R.L. and Arviso, M. "Design studies for the transmission simulator method of experimental dynamic substructuring". In *international seminar on modal analysis (ISMA2010), Lueven, Belgium* (2010)
8. Mayes, R., Rixen, D., Griffith, D., De Klerk, D., Chauhan, S., Voormeeren, S., and Allen, M. "Topics in experimental dynamics substructuring and wind turbine dynamics, volume 2: Proceedings of the 30th imac, a conference on structural dynamics". In *Proceedings of the 30th IMAC, A Conference on Structural Dynamics*, volume 2, pages 21–31. Springer (2012)
9. Crane, N., Day, D., Dohrmann, C., Stevens, B., Lindsay, P., Plews, J., Vo, J., Bunting, G., Walsh, T., and Joshi, S. "Sierra/sd-user's manual-5.10". Technical report, Sandia National Laboratories (2022)
10. Rohe, D.P. *SDynPy* (2021) https://github.com/sandialabs/sdynpy.
11. Adams, B. et al. *Dakota 6.18.0 documentation* (2023) Technical Report SAND2023-03367O, Sandia National Laboratories, Albuquerque, NM.
12. Design, G. "Granta mi" (2023) Software. https://www.grantadesign.com/.